A Comparison of Vibro-Acoustic Modelling Techniques for Resonance Changer Tuning

Paul Dylejko (1), Sascha Merz (2), Nicole Kessissoglou (2) and James Forrest (1)

(1) Maritime Platforms Division, Defence Science and Technology Organisation, Fishermans Bend VIC 3207, Australia
(2) School of Mechanical and Manufacturing Engineering, The University of New South Wales, Sydney NSW 2052, Australia

ABSTRACT

A resonance changer is a device which may be installed in the propulsion system of a marine vessel to reduce the axial vibration transmission from the propeller to the hull. This device is a hydraulic system incorporated in the thrust bearing, which operates analogously to a Helmholtz resonator. Previous work by the authors has examined optimisation of the resonance changer parameters to reduce the acoustic signature of maritime platforms. In those studies, prediction of the low frequency axisymmetric structure-borne noise was carried out using both analytical and fully coupled finite-element/boundary-element models. This paper further develops the analytical model, by including a description of the propeller radiation and its coupling with the hull. The sound power is expressed as the combination of sound radiation from the hull and the direct dipole sound radiation from the propeller. Results calculated from both models are presented for comparison and discussed.

INTRODUCTION

Minimisation of the vibro-acoustic response of maritime vessels improves passenger comfort, minimises crew fatigue and reduces the susceptibility of military platforms. Maritime vessels are dynamically excited by flow noise, on-board machinery and the propulsion system. The low frequency acoustic signature is dominated by on-board machinery and propulsion noise. The propulsion system (for a propeller driven craft) is excited by axial oscillations at the propeller due to its rotation through an unsteady wake. The excitaton is dominated by tonals at the blade-rate and its harmonics (Jiang et al. 1992). The fluctuating forces transmitted along the propeller-shafting system (PSS) results in excitation of the hull and subsequent sound radiation. The pressure field generated by the propeller also excites the hull as well as radiating directly to the far-field.

Transmission of axial vibration through marine propulsion systems has been examined by various researchers. The aim of these studies has been to reduce the vibration transmission to the hull (Pan et al. 2002; Goodwin 1960; Lewis et al. 1989; Rigby 1948). A hydraulic thrust meter used in marine thrust bearings known as the Michell Thrustmeter was found to reduce the severity of some resonance conditions. Further investigation established that the device was acting as a dynamic vibration absorber in transmission (Goodwin 1960). For the purpose of reducing axial vibration in marine propulsion systems, Goodwin renamed the device a resonance changer (RC). The RC introduces elastic, damping and inertial influences by hydraulic means. Dylejko et al. (2007a) investigated the tuning of a RC to minimise the force transmission and time-averaged power transmission from the propeller to the pressure hull of a submerged vessel. The hull was modelled as a simplified 1-D rod, with its mass density adjusted to maintain neutral buoyancy. This work was later extended, by approximating the hull as an axisymmetric fluid-loaded ring-stiffened cylindrical shell (Dylejko et al., 2007b). The RC was tuned, by minimising the maximum radiated sound pressure in the far-field, considering all aspects. More recently, Merz et al. (2010) optimised the RC parameters in a submerged vessel using a fully coupled finite-element/boundary-element (FE/BE) model. The cost function for this study was the radiated sound power. A comparison of the analytical and computational hull models used by Dylejko et al. (2007b) and Merz et al. (2010) respectively was given by Merz et al. (2007).

This paper analytically and computationally investigates the effect of a RC on the radiated sound power of a submerged vessel under axial excitation from the propeller. The forces that arise from the operation of the propeller in a non-uniform wake are transmitted to the hull through both the propeller shaft and the fluid. The combination of the structural and acoustic path has not been considered in previous analytical work. Furthermore, the radiated sound power of the vessel due to both sound radiation from the hull and direct sound radiation from the propeller is presented. Dynamic models of a submerged hull and PSS are developed, using both an analytical model and a fully coupled finite element/boundary element model. The submerged hull is modelled as a fluid-loaded, ring-stiffened, cylindrical shell, with rigid end enclosures. The hull is divided into a number of compartments, separated by bulkheads. Lumped masses are located at each end to represent ballast tanks, which maintain a condition of neutral buoyancy. In the low frequency range (up to 100 Hz), only the hull accordion motion and axial vibration of the PSS are examined, which gives rise to an axisymmetric case. A dynamic model of the PSS including the resonance changer is developed and coupled to the hull models. The sound pressure radiated to the far-field and subsequently the sound power is derived using approximate solutions to the Helmholtz integral equation.

ANALYTICAL MODEL OF A SUBMERGED VESSEL

Substructure dynamic model

A schematic diagram of the proposed substructure model for a submerged vessel is given in Figure 1 (Dylejko et al., 2007b). The velocities at the propeller, shaft, thrust bearing, resonance changer, foundation and hull are described by v_p, v_s, v_b, v_r, v_f and v_h, respectively, while the forces at these locations are given by f_p, f_s, f_b, f_r, f_f and f_h.

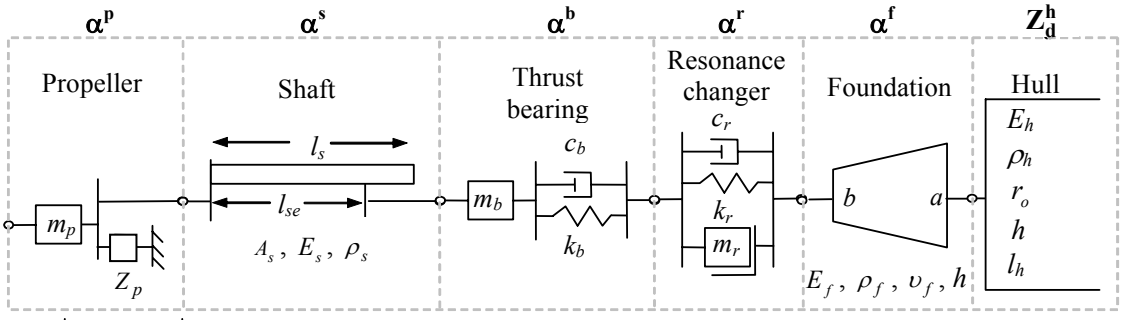

Figure 1. Substructure model of submerged vessel.

The dynamics of the propeller, shaft, thrust bearing, resonance changer and foundation are described by their tranmission matrices, $\boldsymbol{\alpha}^{\mathbf{p}}$, $\boldsymbol{\alpha}^{\mathbf{s}}$, $\boldsymbol{\alpha}^{\mathbf{b}}$, $\boldsymbol{\alpha}^{\mathbf{r}}$ and $\boldsymbol{\alpha}^{\mathbf{f}}$. The hull is represented by a drive-point impedance Z_d^h. Full expressions for the dynamic models used in this paper are given by Dylejko (2007b). In the dynamic models, the time dependence of force and velocity is assumed to be proportional to $e^{-j\omega t}$, where $j=\sqrt{-1}$, ω is the radian frequency and t is time. Modifications to the propeller dynamic model are given in what follows, these account for the external fluid loading.

The propeller is modelled as a lumped mass, which is coupled to both the PSS and surrounding fluid. The fluid loading on the propeller is expressed as a drive-point impedance Z_p and is given in the following section on the propeller pressure field. This impedance term is added to the mass term in the transmission matrix description given by Dylejko (2007b). The propeller is attached to a continuous model of the shaft, which is described by cross sectional area A_s, Young's modulus E_s, density ρ_s and length l_s. Since the response at a point along the shaft corresponding to the location of the thrust bearing is required, an effective length l_{se} is defined. The thrust bearing is represented by a spring-mass-damper system of linear stiffness k_b, damping coefficient c_b and mass m_b.

In this work, a dynamic model of the RC formulated by Goodwin (1960) is used. This model assumes that the fluid flow in the RC is laminar and the pressure-loss calculation may be applied to accelerating flow. The resonance changer exhibits inertial, elastic and damping properties represented by m_r, k_r and c_r, respectively. The symbol used for m_r in Figure 1 indicates that the inertial force is proportional to the relative motion of its two opposing terminals. Figure 2 shows a simplified representation of the RC, which consists of a piston with cross sectional area A_0, oil reservoir with volume V_1 and a connecting pipe with cross-sectional area and length of A_1 and L_1 respectively.

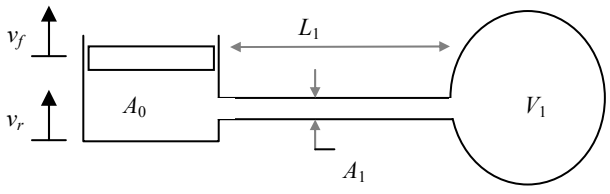

Figure 2. Simplified model of resonance changer.

The virtual mass, stiffness and damping parameters are given by (Goodwin 1960)

$$m_r = \frac{\rho_1 A_0^2 L_1}{A_1}, \quad k_r = \frac{A_0^2 B_r}{V_1}, \quad c_r = 8\pi\mu_1 L_1 \frac{A_0^2}{A_1^2} \tag{1}$$

These parameters are respectively associated with the force required to overcome the inertia of the oil in the pipe, the force required to compress the oil in the reservoir, and the viscous resistance of the oil in the pipe. ρ_1, μ_1 and B_r are respectively the density, viscosity and bulk modulus of the oil contained within the RC system.

For this work, the foundation has been approximated by a linear stiffness connecting fore and aft lumped masses. This is considered to be a valid approximation in the low frequency range (frequencies lower than the first flexural mode of the foundation). The values for these parameters were obtained by fitting this approximation to obtain the same fundamental propeller-shafting resonance as the computational model.

The hull has been modelled as a fluid-loaded, ring-stiffened, cylindrical shell. Both a distributed mass and lumped masses were included to represent the on-board equipment and fore and aft ballast tanks respectively. Bulkheads were modelled as thin circular plates. The bow and stern were simplified as rigid end plates. The full derivation of the hull model is given by Dylejko (2007b). In this work, fluid loading of the end casings has been introduced. This was achieved by including the radiation mechanical impedance Z_e in the appropriate equilibrium equations. Z_e is described in more detail in a later section (End casing pressure field).

The combined response of the complete PSS is given by a 2×2 transmission matrix $\boldsymbol{\beta}^{ps}$ and may be determined by the forward matrix multiplication of the respective transmission matrices $\boldsymbol{\alpha}$ of the different substructures. The expression is given by (Dylejko 2007b)

$$\boldsymbol{\beta}^{ps} = \boldsymbol{\alpha}^{\mathbf{p}}\boldsymbol{\alpha}^{\mathbf{s}}\boldsymbol{\alpha}^{\mathbf{b}}\boldsymbol{\alpha}^{\mathbf{r}}\boldsymbol{\alpha}^{\mathbf{f}} \tag{2}$$

The force transmitted through the PSS to the hull, f_h, resulting from a unit load at the propeller is defined as a function of $\boldsymbol{\beta}^{ps}$ and the hull drive-point impedance Z_d^h as follows (Dylejko 2007b).

$$f_h = \left(\beta_{11}^{ps} + \frac{\beta_{12}^{ps}}{Z_d^h}\right)^{-1} \tag{3}$$

Hence, the PSS may be replaced with a complex force f_h acting on the pressure hull. Furthermore, the propeller velocity resulting from a unit propeller load is given by (Dylejko 2007b)

$$v_p = \left(\beta_{21}^{ps} + \frac{\beta_{22}^{ps}}{Z_d^h} \right) f_h \tag{4}$$

Cylindrical hull pressure field

The far-field radiated sound pressure due to axisymmetric vibration of the hull p_h is given by (Junger and Feit 1985)

$$p_h(R_h, \theta_h) = \frac{j\rho_{fl}\omega^2 e^{jk_f R_h} \tilde{w}(k_f \cos\theta_h)}{\pi k_f R_h \sin\theta_h \, \mathrm{H}_1(k_f r_h \sin\theta_h)} \tag{5}$$

where R_h, r_h, ρ_{fl}, θ_h and k_f are respectively the field-point radius from the cylinder centre, hull radius, fluid density, azimuth with reference to the centre of the cylinder and the fluid wavenumber. $\mathrm{H}_1(k_f r_h \sin\theta_h)$ is the Hankel function of order 1 and $\tilde{w}(k_f \cos\theta_h)$ is the spatial Fourier transform of the axial dependence of the radial displacement, evaluated at $k_f \cos\theta_h$ and is defined as

$$\tilde{w}(k_f \cos\theta_h) = \int_{-L/2}^{L/2} w_h(x_0) e^{-jk_f \cos\theta_h x_0} dx_0 \tag{6}$$

where w_h is the radial displacement of the hull, L is the length of the cylinder and x_0 is the axial coordinate with its origin at the centre of the cylinder.

End casing pressure field

Dylejko (2007b) assumed that the sound radiation from the hull end plates is approximated by adding half the response of a freely suspended piston to half the response of a piston in an infinite baffle, which results in

$$\begin{aligned} p_e = j\omega\rho_{fl} S \, [& - g(R_1)(D_b(\theta_1) + Z_f D_f(\theta_1)) \, \dot{u}_{e1} \\ & + g(R_2)(D_b(\theta_2) + Z_f D_f(\theta_2)) \dot{u}_{e2}] \end{aligned} \tag{7}$$

The subscripts 1 and 2 refer to the stern and bow respectively. $\dot{u}_{e1,2}$ are the rigid body velocities of the end plates. $S = \pi r_h^2$ is the radiating surface area of the end plate. $g(R_{1,2}) = -e^{jk_f R_{1,2}} / 4\pi R_{1,2}$ is the free space Green's function. $R_{1,2}$ are the field-point radii from the radiating surfaces, in this case, the centre of the end plates. $\theta_{1,2}$ are the azimuths with reference to the centre end plates. D_b and D_f are given by

$$D_b(\theta_{1,2}) = \frac{2J_1(k_f r_h \sin\theta_{1,2})}{k_f r_h \sin\theta_{1,2}} \tag{8}$$

$$D_f(\theta_{1,2}) = \frac{2J_1(k_f r_h \sin\theta_{1,2})}{k_f r_h \tan\theta_{1,2}} \tag{9}$$

where J_1 is a Bessel function of the first kind, order 1. The normalised mechanical impedance of the radiation load on a free disk Z_f can be approximated by (Mellow and Kärkkäinen 2005)

$$Z_f = (G_r + jB_r)^{-1} \tag{10}$$

with

$$\begin{aligned} G_r = & 1 + \frac{J_1(2k_f r_h)}{k_f r_h} - 2J_0(2k_f r_h) - \\ & \pi(J_1(2k_f r_h)\mathbf{H}_0(2k_f r_h) - J_0(2k_f r_h)\mathbf{H}_1(2k_f r_h)) \end{aligned} \tag{11}$$

and

$$B_r = \frac{2k_f r_h \mathbf{H}_1(2k_f r_h)}{(k_f r_h - J_1(2k_f r_h))^2 + (\mathbf{H}_1(2k_f r_h))^2} \tag{12}$$

$\mathbf{H}$ is the Struve function. The mechanical impedance of the end casings Z_e is approximated by half the mechanical impedance of a free rigid disk

$$Z_e = \rho_{fl} c_f S Z_f \tag{13}$$

This expression follows from the approximation used to calculate the sound radiation from the end casings.

Propeller pressure field

The propeller sound field is dominated by sound radiation due to (i) the hydrodynamic mechanism that arises through the propeller operating in a non-uniform wake and (ii) the axial fluctuation of the propeller due to vibration of the shafting system. Hence, the sound field due to rotating thrust and blade-thickness which results in rotating monopoles and dipoles has been neglected in the following analysis. The sound radiation originates from the propeller blades as multiple dipoles. The dipoles can be simplified to a single dipole located at the propeller hub, because the wavelength is large relative to the propeller diameter and the propeller is small relative to the hull. A derivation of the dipole field pressure due to a fluctuating force is provided by Ross (1987). The directivity pattern of the dipole is governed by cos β, where β is the angle between the field point vector with respect to the source and the force direction. The dipole amplitude is directly proportional to the structural force. The radial variation of the amplitude follows $1/R_p$ in the near field and $1/R_p^2$ in the far field, where R_p is the field-point radius from the propeller. The transition is a function of the wavelength λ and occurs at $\lambda/2\pi$.

For (i), corresponding to the sound radiation due to the hydrodynamic mechanism, the sound radiation due to the force on the propeller hub is

$$p_p(R_p, \theta_p) = jk_f f \, g(R_p) \left(1 - \frac{j}{k_f R_p} \right) \cos\theta_p \tag{14}$$

where f is the amplitude of the exciting force. θ_p denotes the angle between the hull axis and the vector pointing from the propeller hub to the field point, at which the pressure is evaluated. For (ii), corresponding to propeller vibration, the propeller was simplified to a rigid circular disc. The problem reduces to a dipole according to equation (14) for small values of the Helmholtz number $k_f a_p$, where a_p is the disc

radius (propeller radius). The axial velocity v_p of the propeller can be related to the equivalent force by an impedance

$$Z_p = \frac{f}{v_p} = 2\pi a_p^2 Z_f Z_a \tag{15}$$

where Z_a is the characteristic impedance of the fluid.

The excitation of the hull by the propeller-field has been included in this work. The far-field approximation has been used to calculate the pressure over the stern end casing. Assuming perfect reflection, which results in twice the pressure at a rigid boundary, an additional force can be included on the stern of the hull. This force was evaluated by integrating the resulting pressure over the stern end plate. When the separation of the propeller and the stern end of the pressure hull is much larger than the propeller radius, this approximation is reasonable.

Radiated sound power

Under the assumption that there is little interaction between the radiating surfaces, the total far-field radiated sound pressure p_T may be approximated by adding the contributions of each surface. For an inviscid acoustic medium, the radiated acoustic power from a source is independent of range. Utilising this independence, the sound power can be obtained from the far-field radiated sound pressure. Consequently, the time averaged radiated sound power can be given as (Wu 2000)

$$\Pi = \frac{\pi R_h^2}{\rho_f c_f} \int_0^{\pi} \left| p_T(R_h, \theta, f_h) \right|^2 \sin\theta_h \, \mathrm{d}\theta_h \tag{16}$$

COMPUTATIONAL MODEL OF A SUBMERGED VESSEL

The computational FE/BE model includes both the propeller/shafting system and the submerged hull (Merz 2010). The acoustic properties of the propeller are modelled using a semi-analytical approach, which was described in the previous section (Propeller pressure field). The structural properties of the propeller/shafting system and the submerged hull are modelled using finite elements. The acoustic properties of the submerged hull are modelled using boundary elements.

Coupled FE/BE modelling

For the computational model, finite elements have been used to represent the structural domain. The dynamic finite element formulation has been derived by assuming linear elasticity. The cylindrical pressure hull, the bulkheads and the foundation of the propeller shafting system were represented by axisymmetric shell elements based on Kirchhoff-Love theory or Reissner-Mindlin theory, respectively. Ring stiffeners with a rectangular cross-section were considered using shell elements. Details on the FE modelling and the FE meshes have been presented by Merz (2010).

The end plate is rigid and therefore its grid resolution has no influence on the results. As the joints, especially at the bulkheads and end plates, lead to evanescent near-field waves with a small wavelength, a fine FE mesh is required for convergence of the results in terms of the natural frequencies and displacements.

One-dimensional finite elements were used to model the dynamics of the propeller/shafting system, as only axial excitation of the hull was taken into account. Rod elements were used to model the propeller shaft. The lumped masses at the end plates, the propeller structural and fluid loading masses, the mass of the thrust bearing and the virtual mass of the RC were modelled using point masses. The stiffness and damping of both the thrust bearing and the resonance changer have been modelled using spring-damper elements. Using finite elements, the structural domain is represented by the following system of equations (Zienkiewicz and Taylor, 2005)

$$\mathbf{A}\mathbf{u} = \int_{\Gamma} \mathbf{N}_{\Gamma} \mathbf{f}_{\Gamma} \, \mathrm{d}\Gamma + \mathbf{f} \tag{17}$$

where $\mathbf{A}$ is the system matrix for the structure, $\mathbf{u}$ is the nodal displacement vector, $\mathbf{N}$ is the global matrix of interpolation functions at the structural surface Γ, $\mathbf{f}_{\Gamma}$ is the surface traction vector and $\mathbf{f}$ is the vector of nodal forces.

The direct boundary element method has been used to represent the interior and exterior fluid domains by solving the Helmholtz equation. A special BE formulation for axisymmetric problems was employed to reduce computational cost. Details on the BE modelling and the BE meshes have been presented by Merz (2010). Application of the boundary element method results in the following system of equations (Wu, 2000)

$$\mathbf{G}\mathbf{v} + \mathbf{H}\mathbf{p} = \mathbf{p}_{\mathrm{inc}} \tag{18}$$

where $\mathbf{G}$ and $\mathbf{H}$ are the BE system matrices, $\mathbf{v}$ is the vector of normal velocities at the collocation points and $\mathbf{p}$ is the vector of pressures at the collocation points. The vector $\mathbf{p}_{\mathrm{inc}}$ contains the pressure at the collocation points due to the dipole correlated to the operation of the propeller in a non-uniform wake and is computed using equation (14).

As the dipole pressure $\mathbf{p}_{\mathrm{inc,prop}}$ due to axial propeller fluctuation depends on the axial surface normal velocity of the propeller, it can be expressed in terms of $\mathbf{v}$

$$\mathbf{p}_{\mathrm{inc,prop}} = \mathbf{G}_{\mathrm{prop}} \mathbf{v} \tag{19}$$

The sparse matrix $\mathbf{G}_{\mathrm{prop}}$ is computed using equations (14) and (15) and subtracted from matrix $\mathbf{G}$. The pressure at a set of points in the acoustic domain is obtained by

$$\mathbf{p}_{\Omega} = \mathbf{G}_{\Omega} \mathbf{v} + \mathbf{H}_{\Omega} \mathbf{p} + \mathbf{p}_{\mathrm{inc},\Omega} \tag{20}$$

where $\mathbf{G}_{\Omega}$ and $\mathbf{H}_{\Omega}$ are matrices that arise from integration of Green's function and its normal derivative over the boundary. $\mathbf{p}_{\mathrm{inc},\Omega}$ is a vector of pressure values at the field points due to the incident field.

Strong coupling of the acoustic BE and the structural FE methods is achieved by imposing that (a) the normal velocity of the structure equals the normal velocity of the fluid and (b) the normal distributed surface load of the structure equals the acoustic surface pressure at the structure/fluid interface. For non-conforming meshes at the coupling interface, condition (a) cannot be considered in a strong sense. Therefore, an approach similar to that presented by Belgacem (1999) is used. The pressure can be interpreted as a Lagrange multiplier and continuity of the surface normal velocity is only established in a weak sense (Fritze et al. 2005)

$$\int_{\Gamma} \phi_{\mathrm{f}} v_{\mathrm{f}} \mathrm{d}\Gamma = \int_{\Gamma} \phi_{\mathrm{f}} v_{\mathrm{s}} \mathrm{d}\Gamma \tag{21}$$

where Γ is the fluid/structure interface. The test function ϕ_f corresponds to the global interpolation function for the fluid domain variables. v_f and v_s are the surface normal velocities of the structural and fluid domains, respectively. Equation (21) can be expressed in matrix form as

$$\mathbf{L}_f \mathbf{v} = j\omega \mathbf{L}_s \mathbf{u} \tag{22}$$

Equations (17), (18) and (22) can be combined to form the saddle point problem

$$\begin{bmatrix} \mathbf{A} & \mathbf{L}_s^T & \mathbf{0} \\ \mathbf{0} & \mathbf{H} & \mathbf{G} \\ j\omega\mathbf{L}_s & \mathbf{0} & \mathbf{L}_f \end{bmatrix} \begin{Bmatrix} \mathbf{u} \\ \mathbf{p} \\ \mathbf{v} \end{Bmatrix} = \begin{Bmatrix} \mathbf{f} \\ \mathbf{p}_{inc} \\ \mathbf{0} \end{Bmatrix} \tag{23}$$

When discontinuous boundary elements are used, the matrix $\mathbf{L}_f$ becomes a diagonal matrix and $\mathbf{v}$ can be explicitly expressed in terms of $\mathbf{u}$. The reduced system of equations can then be written as

$$\begin{bmatrix} \mathbf{A} & \mathbf{L}_s^T \\ j\omega\mathbf{L}_f^{-1}\mathbf{L}_s\mathbf{G} & \mathbf{H} \end{bmatrix} \begin{Bmatrix} \mathbf{u} \\ \mathbf{p} \end{Bmatrix} = \begin{Bmatrix} \mathbf{f} \\ \mathbf{p}_{inc} \end{Bmatrix} \tag{24}$$

Radiated sound power

The complex radiated sound power through a surface Λ is given by (Wu 2000)

$$\Pi = \frac{1}{2}\int_{\Lambda} pv^* \, d\Lambda \tag{25}$$

where p is the acoustic pressure of the fluid and v is the normal velocity of a fluid particle at the surface.

If the surface Λ is spherical and in the far-field with respect to the sound sources, equation (25) simplifies to (Ross 1987)

$$\Pi = \frac{1}{2\rho c}\int_{\Lambda} pp^* \, d\Lambda \tag{26}$$

where c is the speed of sound. When Λ is subdivided into polygons and the pressure is expressed as a piecewise linear approximation, then equation (26) can be rewritten as

$$\Pi = \mathbf{p}_\Lambda^H \mathbf{\Phi} \mathbf{p}_\Lambda \tag{27}$$

where $\mathbf{p}_\Lambda$ is the vector of pressures in the vertices of the polygons and the diagonal matrix $\mathbf{\Phi}$ describes the geometry of Λ and the fluid properties. The sound power radiated from the submerged hull is computed by setting $\mathbf{p}_\Lambda = \mathbf{p}_\Omega$, where $\mathbf{p}_\Omega$ is the vector of sound pressure values due to sound radiation from the hull at the integration points for the sphere.

RESULTS

The physical values associated with the submerged hull used in this work are presented in Table 1. The values of the parameters used to model the PSS, including the resonance changer parameters, are given in Table 2. Hysteretic damping was included for the shaft and hull by introducing a complex Young's modulus $E(1-j\eta)$, where $\eta = 0.02$ is the structural loss factor. It was assumed that the stiffeners were made from the same material as the hull. In the following analyses, an axial harmonic load at the propeller of 1 N has been used.

For the analytical model, the propeller pressure field exciting the hull is calculated using the far-field derivation of a free rigid disk. The distance from the propeller to the end casing is 10.079m. Given this distance is a few times larger than the hull radius, this approach is reasonable.

One of the aims of this work is to compare the results obtained from the analytical and computational models. For this reason, the two models were set up to be as similar as possible. One difference however, is that the computational model uses a rigid conical rear casing. While both models considered the fluid loading on the propeller, it should be noted that the computational model did not include the resistive component (radiation damping).

Table 1. Hull parameters

Parameter	Value
Hull radius	3.25 m
Pressure hull length	45 m
Hull thickness	0.04 m
Stiffener cross-sectional area	0.012 m^2
Stiffener spacing	0.5 m
Bulkhead plate thickness	0.04 m
Mass of stern lumped mass	188 tonne
Mass of bow lumped mass	200 tonne
Extra equipment mass per unit area	697.6 kg/m^2
Conical shell length	10 m
Conical shell thickness	0.01 m
Half cone angle	18º
Steel mass density	7800 kg/m^3
Steel Young's modulus	200 GPa
Steel Poisson's ratio	0.3
Density of surrounding fluid	1000 kg/m^3
Speed of sound in the fluid	1500 m/s

Figure 3 compares the radiated sound power predicted from the analytical model without a RC, with and without the propeller pressure field. For the case with the propeller pressure field, the hull has been excited by both the structural path (through the PSS) and the propeller near-field (through the fluid). The peak at 37 Hz corresponds to the fundamental resonance of the PSS (in the absence of a RC). This resonance results in large propeller and hull motion. The other peaks at around 21, 44 and 70 Hz correspond to the first three hull axial resonances. Bulkhead resonances at around 9 and 36 Hz can also be observed. In the absence of a RC, the effect of neglecting the propeller sound field in the prediction of the radiated sound power is minimal below around 75 Hz. For frequencies greater than 75 Hz, a discrepancy of up to 9.7 dB is observed. Including the propeller sound field, leading

to radiation from both the hull and propeller, has the effect of increasing the radiated sound power at higher frequencies.

Table 2. Propeller-shafting system parameters

Parameter	Value
Propeller mass	10 tonne
Shaft cross sectional area	0.0707 m^2
Shaft density	7800 kg/m^3
Shaft Young's modulus	200 GPa
Shaft Poisson's ratio	0.3
Shaft length	10.5 m
Shaft effective length	9 m
Thrust bearing mass	0.2 tonne
Thrust bearing stiffness	20 GN/m
Thrust bearing damping rate	300 tonne/s
Resonance changer stiffness	169 MN/m
Resonance changer mass	1 tonne
Resonance changer damping	287 tonne/s
Foundation stiffness	11 GN/m
Foundation forward mass	710 kg
Foundation aft mass	365 kg

Figure 4 compares the radiated sound power predicted from the analytical model with a RC, with and without the propeller pressure field. Neglecting the propeller sound field when a RC is implemented leads to under-estimation of the radiated sound power by more than 20 dB for frequencies greater than 30 Hz. This result demonstrates the importance of including a propeller radiation model for RC tuning, even in this low frequency regime.

Figure 5 compares the radiated sound power calculated from the analytical and computational models with and without the use of a resonance changer, without the propeller pressure field. Results show that implementation of a RC in the PSS has resulted in a significant reduction of the overall radiated sound power above 25 Hz. However, when a RC is implemented, the fundamental resonance of the PSS has shifted from 37 Hz to 12 Hz, leading to an increase in radiated sound power at lower frequencies. The analytical results exhibit a slightly lower radiated sound power at the propeller shafting resonance than the computational model. This discrepancy is attributed to the computational model ignoring the radiation damping on the propeller. The results from the analytical and computation models, however, show very good agreement over most of the frequency range. The mean difference between the results from the two models was 1.9 dB with the largest deviation of 4.5 dB occurring at 41 Hz for the case without the RC.

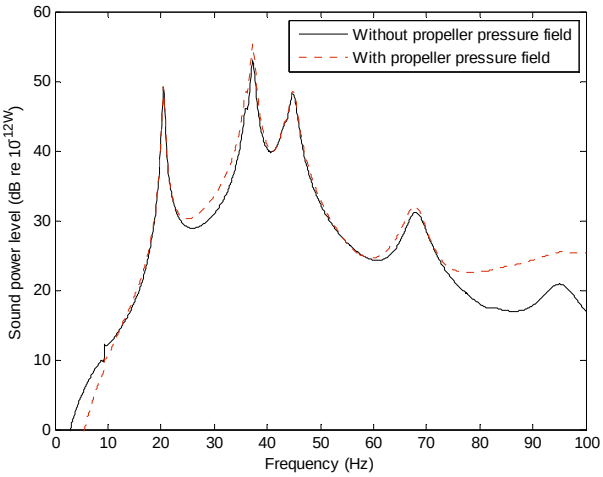

Figure 3. Radiated sound power without a RC, not including the propeller pressure field (solid line) and including the propeller pressure field (dotted line) - analytical results only.

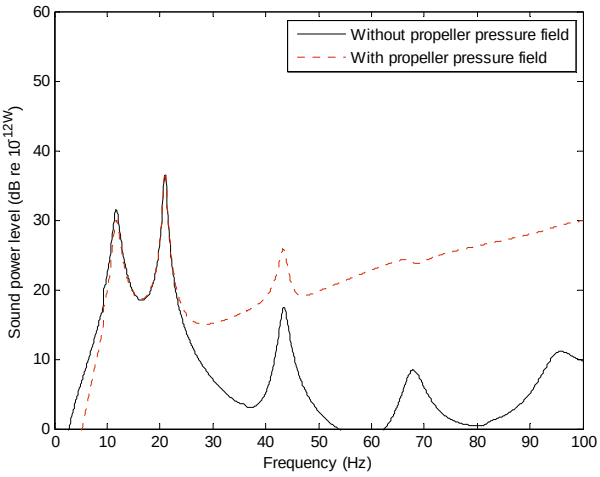

Figure 4. Radiated sound power with a RC, not including the propeller pressure field (solid line) and including the propeller pressure field (dotted line) - analytical results only.

Figure 6 analytically and computationally predicts the radiated sound power with and without the use of a resonance changer, including the propeller sound field. When the propeller sound field is taken into account, the effect of the resonance changer is limited to frequencies below around 70 Hz. The prediction of the performance of the RC is significantly affected by the influence of acoustic radiation from the propeller. Introduction of the RC can provide significant reduction in the overall radiated sound power at frequencies around the original PSS resonance. The RC, however, has a much more limited effect at higher frequencies, where the dipole fields from the propeller tend to be the dominant cause of radiated sound power. The results from the analytical and computational models again compare very well. The maximum difference was 5.1 dB at 47 Hz for the case with the RC. The mean difference was 2 dB. It should be noted that the largest deviations generally occurred at frequencies between resonances.

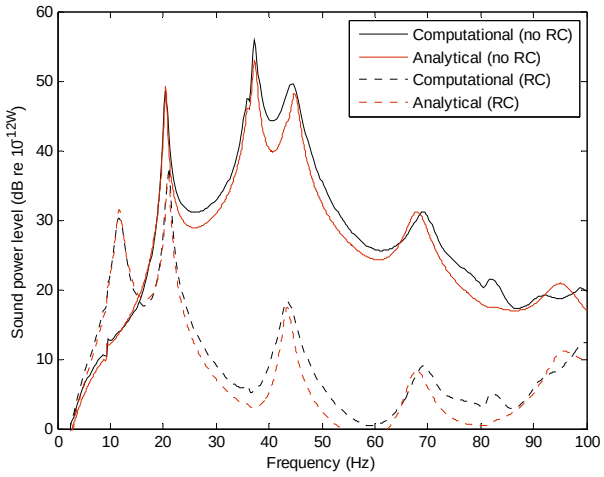

Figure 5. Radiated sound power with (dotted line) and without (solid line) a RC, not including the propeller pressure field.

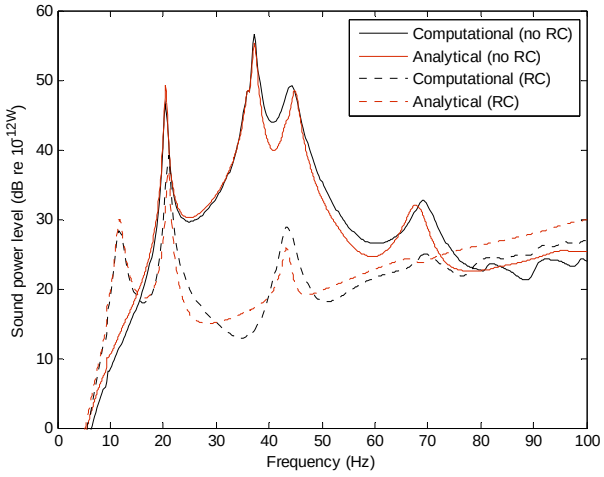

Figure 6. Radiated sound power with (dotted line) and without (solid line) a RC, including the propeller pressure field.

CONCLUSIONS

Analytical and computational results for the prediction of the low frequency (up to 100 Hz) radiated sound power from a fluid loaded submerged vessel have been presented. Axial excitation of the hull from both the PSS and the propeller near-field has been investigated. The contributions to the radiated sound power from the first three axial resonant frequencies of the hull circumferential breathing modes as well as the fundamental resonance of the PSS were observed.

The performance of a hydraulic vibration attenuation system known as a resonance changer (RC) implemented in the PSS has been examined. The RC was shown to provide significant reduction in the total radiated sound power at frequencies around the original PSS resonance. This is achieved by reducing the stiffenss of the PSS, shifting this resonance to a lower frequency. It was found that the predicted reduction in radiated sound power with the introduction of the RC is not as large when the propeller sound field is taken into account. This is associated with the propeller becoming an efficient radiator at higher frequencies. This result demonstrates the importance of incuding a propeller radiation model when tuning a RC to reduce the radiated sound power.

Computational methods can generate more detailed models compared with analytical techniques. This is largely in their ability to model complicated geometries. Analytical models, however, usually execute a solution in a shorter time-frame. This study demonstrates excellent agreement between an analytical and computational model, with a maximum deviation between the two models of 5.2 dB. The maximum mean deviation was 2 dB.

REFERENCES

Belgacem, F.B. 1999, 'The mortar finite element method with Lagrange multipliers', *Numerische Mathematik*, vol. 84, no. 2, pp. 173-197.

Dylejko P.G., Kessissoglou N.J., Tso Y. and Norwood C.J. 2007a, "Optimisation of a resonance changer to minimise the vibration transmission in marine vessels". *Journal of Sound and Vibration*, vol. 300, pp. 101-116.

Dylejko P.G. 2007b, *Optimum resonance changer for submerged vessel signature reduction*. PhD thesis, University of New South Wales, Sydney, Australia.

Fahy, F. 1985, *Sound and Structural Vibration: Radiation, Transmission, and Response,* Academic Press, London, UK.

Fritze, D., Marburg, S. and Hardtke, H.J. 2005, "FEM-BEM-coupling and structural-acoustic sensitivity analysis for shell geometries", *Computers & Structures,* vol. 83, no. 2-3, pp. 143-154.

Goodwin A.J.H. 1960, "The design of a resonance changer to overcome excessive axial vibration of propeller shafting". *Transactions of the Institute of Marine Engineers*, vol. 72, pp. 37-63.

Jiang C.-W., Chang M. and Liu Y. 1992, "The effect of turbulence ingestion on propeller broadband forces". *Proceedings of the 19th Symposium on Naval Hydrodynamics*, Seoul, Korea, pp. 751-769.

Junger, M.C. and Feit, D. 1985, *Sound, structures and their interaction*, MIT Press.

Lewis D.W., Allaire P.E. and Thomas P.W. 1989, "Active magnetic control of oscillatory axial shaft vibrations in ship shaft transmission systems, part 1: System natural frequencies and laboratory scale model", *Tribology Transactions*, vol. 32, pp. 170-178.

Mellow, T. and Kärkkäinen, L. 2005, "On the sound field of an oscillating disk in a finite open and closed circular baffle", *Journal of the Acoustical Society of America,* vol. 118, no. 3, pp. 1311-1325.

Merz, S. 2010, *Passive and Active Control of the Sound Radiated by a Submerged Vessel due to Propeller Forces*, PhD Thesis, The University of New South Wales, Sydney, Australia.

Merz, S., Kessissoglou, N.J., Kinns, R. and Marburg, S. 2010, "Minimisation of the sound power radiated by a submarine through optimisation of its resonance changer", *Journal of Sound and Vibration,* vol. 329, pp. 980-993.

Merz, S., Oberst, S., Dylejko, P. G., Kessissoglou, N. J., Tso, Y. K. and Marburg, S. 2007, "Development of coupled FE/BE models to investigate the structural and acoustic responses of a submerged vessel", *Journal of Computational Acoustics*, vol 15, pp 23-47.

Pan J., Farag N., Lin T. and Juniper R. 2002, "Propeller induced structural vibration through the thrust bearing". *Proceedings of Acoustics 2002*, Adelaide, Australia, pp. 390-399.

Rigby C.P. 1948, “Longitudinal vibration of marine propeller shafting”, *Transactions of the Institute of Marine Engineers*, vol. 60, pp. 67-78.

Ross, D. 1987, *Mechanics of Underwater Noise,* Penninsula Publishing, Los Altos, CA.

Wu, T.W. editor, 2000, *Boundary Element Acoustics*, WIT Press, Southampton, UK.

Zienkiewicz, O.C. and Taylor, R.L. 2005, *The Finite Element Method: Its Basis and Fundamentals*, Volume 1, Elsevier Butterworth-Heinemann, Amsterdam, Netherlands, 6th edition.